

Reuse your features: unifying retrieval and feature-metric alignment

Javier Morlana and J.M.M. Montiel

Abstract—We propose a compact pipeline to unify all the steps of Visual Localization: image retrieval, candidate re-ranking and initial pose estimation, and camera pose refinement. Our key assumption is that the deep features used for these individual tasks share common characteristics, so we should reuse them in all the procedures of the pipeline. Our DRAN (Deep Retrieval and image Alignment Network) is able to extract global descriptors for efficient image retrieval, use intermediate hierarchical features to re-rank the retrieval list and produce an initial pose guess, which is finally refined by means of a feature-metric optimization based on learned deep multi-scale dense features.

DRAN is the first single network able to produce the features for the three steps of visual localization. DRAN achieves a competitive performance in terms of robustness and accuracy specially in extreme day-night changes.

I. INTRODUCTION

Feature extraction is a relevant step in most of computer vision tasks. Traditional approaches rely on image gradients to extract *sparse features*, for example, edges or keypoints in a fixed hand-crafted manner. In the last decade, deep learning has taken the spot in feature extraction, with Convolutional Neural Networks (CNNs) as the most successful method. CNNs apply a set of convolutional filters to the image, obtaining a *dense hierarchy of features*. Inherently, CNNs go deeper as the resolution decreases while obtaining higher semantics, obtaining a pyramidal representation of the image.

In this work, we focus on visual localization for visual SLAM (Simultaneous Localization And Mapping from visual sensors), i.e, we are assuming that a 3D map of the scene is available, which has been built using SfM (Structure-from-Motion) or Visual SLAM. The map is composed of 3D points, \mathbf{P}_i , and keyframes. Keyframes, also called reference frames, are a selected set of images from which the map geometry is computed by bundle adjustment. Per each keyframe, we have available its image \mathbf{I}_j and its camera pose $\{\mathbf{R}_j, \mathbf{t}_j\}$

Given a query image \mathbf{I}_q and the map, the goal of camera location is to efficiently retrieve the closest map keyframes, \mathbf{I}_k , and the 6-DoF pose of the query image with respect to the map, $\{\mathbf{R}_q, \mathbf{t}_q\}$.

First we apply a *keyframe retrieval step*, in which the typical deep learning retrieval algorithm usually takes three sub-steps: i) the query image is forwarded through the network encoder, a dense hierarchy of features, ii) the deepest

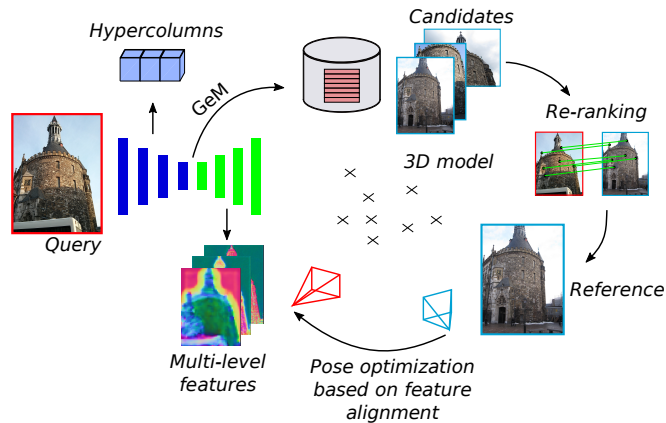


Fig. 1: In a single forward pass our DRAN network extracts a unique hierarchy of features to perform: image retrieval, candidate re-ranking and feature-metric pose estimation. The image retrieval gives the most similar keyframes to the query in a given 3D map. This list of candidates is re-ranked by the matching of hypercolumns from the encoder. The top keyframe after re-ranking gives the initial 6 DoF pose guess which is refined through feature-metric optimization.

feature map is pooled [1, 2] obtaining a compact global descriptor, and iii) the descriptor is compared against the other global descriptors of the keyframes in the database, ranking the keyframes by descriptor similarity. Images are translated into compact vectors based on the deepest features, which typically encodes the high-level features of the image. The comparison of global descriptors gives an initial list of candidate keyframes ranked by similarity.

For the *camera feature-metric pose estimation step*, we apply deep image alignment techniques [3–6] minimizing a feature-metric error of the dense hierarchical features that encode the image at different resolutions, estimating the relative pose between the query and a keyframe. These methods are robust against illumination and point of view changes, and achieve high precision as they can get subpixel accuracy, but they need a good initial pose guess to converge to the correct minimum.

Most of the candidate keyframes in the list depict the same place as the query and might provide a coarse pose initialization to the feature-metric optimization, but their sorting criteria does not take into account the conditions that most favour the pose optimization, i.e. point of view similarity. For this reason, the intermediate *re-ranking step* re-sort the keyframes in the initial list to prioritize the overlap and point of view similarity with the query. This

This work was supported by the EU-H2020 grant 863146: ENDOMAPPER, the Spanish government grants PGC2018-096367-B-I00, and by Aragón government grant DGA_T45-17R.

The authors are with the Instituto de Investigación en Ingeniería de Aragón (I3A), Universidad de Zaragoza, María de Luna 1, 50018 Zaragoza, Spain. E-mail: {jmorlana, josemari}@unizar.es.

step exploits the dense hierarchy of features to produce matches between the query and the keyframes that yield 2D-3D matches between the query and the map which are refined by a PnP RANSAC. After this step, we have an initial pose guess which is closer to the true one, and the feature-metric optimization can successfully converge.

Other works in literature deal with camera location employing different networks for each of the steps. In contrast to them, we use a unique dense hierarchy of features what is efficient and elegant, providing competitive results of accuracy.

Our key insight is that it is beneficial to use a unique hierarchy of learned features for all the steps of the camera visual localization. Following these ideas, we propose DRAN (Deep Retrieval and image Alignment Network, Figure 1), a unified architecture that combines the knowledge from retrieval and camera pose stages. Our contributions are:

- DRAN, a multi-task single network providing, in a single forward pass, both an image global descriptor for retrieval, hypercolumns for re-ranking and initial pose estimation, and a multi-level dense feature hierarchy for feature-metric camera pose refinement.
- We demonstrate that well-localized features are already present in image retrieval networks, so there is no need to train two separate pipelines for the tasks of retrieval and localization.
- An evaluation under challenging conditions, showing that our system achieves better performance than other unified systems, and it is competitive against feature matching pipelines that combine different networks.

II. RELATED WORK

We review the relevant work in the related areas of this paper: direct and indirect SLAM, image retrieval, deep camera pose estimation and unified methods.

Direct and Indirect SLAM is the widely used classification for traditional SLAM techniques. Indirect SLAM [7–10], processes the image to detect, describe and match a sparse set of keypoints that are robust to illumination and viewpoint changes, these matches are fed in a geometric Bundle Adjustment to recover the scene geometry. In contrast, direct SLAM operates with raw image intensities, relying on brightness consistency [11–13] to also feed, in this case, a photometric Bundle Adjustment. Direct alignment allows sub-pixel accuracy but is vulnerable to illumination changes and suffers from small convergence basin. We propose the use of learned features to overcome the challenges of the direct methods when applied to camera pose estimation.

Image retrieval stands for the task of efficiently retrieve an image among a database of visited places, in our case the keyframes. To perform a quick search, a compact image representation is needed. Before the advent of deep learning, the image embedding was obtained by the aggregation of hand-crafted local descriptors such as SIFT [14], ORB [15] in a Bag-of-Words [16, 17] representation. Nowadays, the field is dominated by CNN representations that aggregate feature maps into a global descriptor [1, 2, 18–20]. Thanks

to this embedding, two images can be compared efficiently with a single distance computation between descriptors. Our work adopts the state-of-the-art pooling method GeM for the image retrieval step[1].

Deep camera pose estimation mainly encompassed three approaches: pose regression, image matching and deep direct alignment. Pose regression [21, 22] learns to directly map the input to pose parameters without any 3D constraint. They require a lot of training data and don’t generalize well to novel domains. Differently, image matching extracts local features [23–25] and perform data association by descriptor distance or learned matchers [26, 27]. The pose can be obtained with a PnP [28] algorithm if those local features are present in a 3D reference model. Deep direct alignment [3–6, 29] takes an approach similar to direct SLAM, trying to minimize a photometric error based on the deep features of a CNN, i.e. a feature-metric optimization. In this work, we build on top of the recent framework PixLoc [3], which extracts multi-scale dense descriptors that are aligned iteratively in a pyramidal approach. The feature-metric error is evaluated on the 2D projections of the corresponding 3D model built by Structure-from-Motion. S2DNet [30] is another approach that also takes advantage of the map projections to match sparse deep descriptors from the reference frame against the dense descriptors of the query. In contrast to us, S2DNet is trained to solve only the matching step between two images.

Unified approaches trying to join the local and global descriptor extraction into a single system can be found in the literature. DELG [31] obtains the GeM global descriptor provided by [1] and applies an attention mechanism [32] to obtain a descriptor that reranks the initial retrieval candidates. HF-Net [25] proposed a distillation framework in a teacher-student approach to learn from NetVLAD [2] and SuperPoint [23], being able to perform retrieval and camera localization. UR2KiD [33] also performs retrieval and matching, with the benefit of being trained only with image labels. S2DHM [34] uses an encoder pretrained for retrieval to perform re-ranking and extract an initial pose under challenging conditions. We use the ideas of S2DHM but applying them to a networks trained in a generic retrieval datasets (SfM120k [1]). Besides, differently from them, our work unifies the tasks of image retrieval, local matching and feature-metric image alignment, introducing, to the best of our knowledge, the first system to combine them in the same network.

III. FEATURE HIERARCHY FOR RETRIEVAL AND ALIGNMENT

In this section, we detail the steps of visual localization using a single network, giving birth to our *Deep Retrieval and Image Alignment Network*.

A. Deep Retrieval and Image Alignment Network

We propose DRAN (Deep Retrieval and image Alignment Network) architecture, whose main steps are described in Fig. 2. We argue that most of the meaningful features are already extracted by image retrieval networks, so we don’t need to train another full pipeline end-to-end to detect the

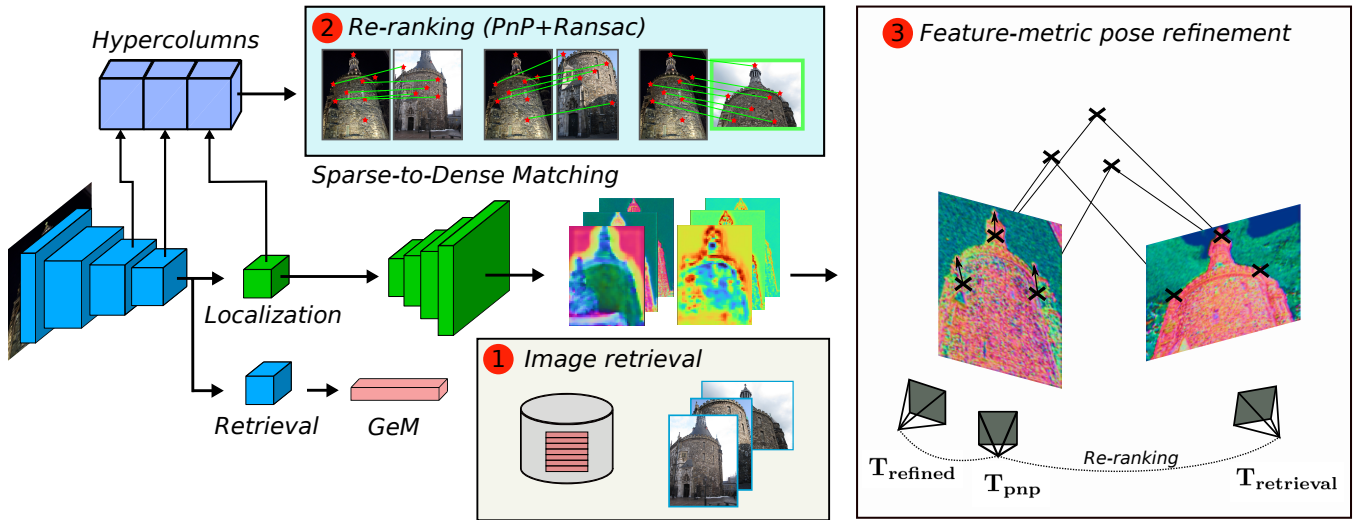


Fig. 2: **DRAN pipeline.** DRAN provides the features for the three steps of Visual Localization with a single network. The architecture follows a UNet style with two heads: localization and retrieval. The blocks shown in green are trained specifically for feature-metric alignment, while the ones shown in blue are pretrained in a generic retrieval dataset and frozen during training.

features for the image alignment that estimates the camera pose. For this purpose, we adopt a shared encoder architecture with two heads: retrieval and localization. The shared encoder is a VGG16 encoder pretrained for image retrieval in the SfM120k dataset, which is splitted after the `conv4` stage. We use SfM120k to pretrain our encoder. This kind of data is easier to obtain than accurate 3D models and allows to acquire invariance against challenging conditions.

The retrieval head incorporates the last stage of the truncated encoder (`conv5`) and a Generalized-Mean pooling layer that aggregates the last feature map into a compact vector. As we don't want to affect the retrieval performance, both the shared encoder and the retrieval head remain frozen during the training stage, retaining their original weights fine-tuned for retrieval.

The localization head has identical structure as the retrieval head (`conv5` of VGG16), with the difference that it is optimized during training (Figure 4). It connects to a decoder network with skip connections in a UNet style. Following [3], we optimize all the weights involved in order to learn features for accurate camera localization (III-D). The output of the decoder is the hierarchy of features, along with its uncertainty. The representation of an image for each scale level l is a feature map $\mathbf{F}^l = \mathbb{R}^{W_l \times H_l \times D_l}$ and its per pixel uncertainty $\mathbf{U}^l = \mathbb{R}^{W_l \times H_l}$. The decoder also feeds the estimator for the damping factor of the Levenberg-Marquardt feature-metric optimization.

To provide a good initial guess for the feature-metric camera pose optimization, we extract hypercolumns [34] using the already computed features of the shared encoder and the localization head. This allows us to filter the retrieval candidates and obtain an initial pose by means of a PnP-Ransac. This pose is better than the coarse pose obtained by image retrieval, boosting the localization performance of the

subsequent optimization.

B. Compact Global Image Descriptor

We adopt the Generalized-Mean (GeM) [1] pooling layer as the method to aggregate the activations from the last layer of the retrieval head. The GeM operation for each channel of the $C \times H \times W$ activation maps is described as

$$\mathbf{f} = [f_1 \dots f_k \dots f_K]^\top \in \mathbb{R}^{512}, \quad f_k = \left(\frac{1}{|\mathcal{X}_k|} \sum_{x \in \mathcal{X}_k} x^{p_k} \right)^{\frac{1}{p_k}} \quad (1)$$

Where \mathcal{X}_k is the set of HW activations of each channel and p_k is the learnt parameter that controls the pooling operation. Both the encoder and p_k is trained in the SfM120k [1] dataset, which depicts popular landmarks clustered by COLMAP. It is trained using a siamese architecture and the contrastive loss. The contrastive loss takes as input a tuple containing 1 query, 1 positive example and 5 negative examples. Here the objective is to obtain similar descriptors for images depicting the same place, where the distance is computed by the dot product of two L2-normalized global descriptors.

C. Re-ranking and initial pose estimation

The image retrieval module focuses on finding keyframes depicting the same place than the query, but in some cases, the first candidate is not the best initialization for feature-metric alignment. Images can suffer from big changes in scale or in the point of view, or little overlap, resulting in a bad pose initialization than can hinder convergence to the optimal pose.

For this reason, we employed a re-ranking method that minimize this issue by selecting the best candidate to initialize with, based on the number of inliers. We brought the

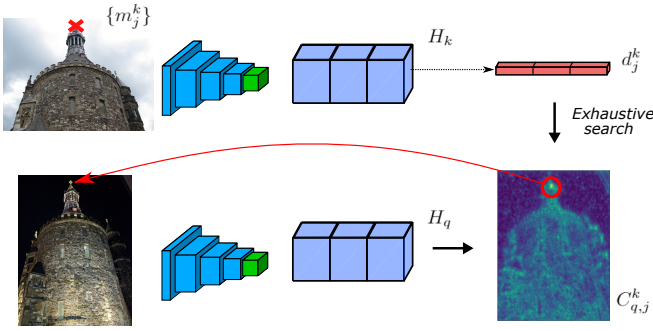


Fig. 3: Exhaustive matching for re-ranking and initial pose. We only attempt to match points present in the map, obtaining a sparse set of descriptors from the dense hypercolumn H_k . Each descriptor d_j^k is searched densely in the query hypercolumn H_q , identifying the match as the global maxima of the cross-correlation map.

method S2DHM (Sparse-to-Dense Hypercolumn Matching) proposed by Germain et al. [34] to our features. The goal is to obtain local matches between the query and the keyframes with the features extracted by the encoder, in order to filter the image retrieval candidates and estimate an initial 6DoF pose guess.

Given a query I_q and a keyframe I_k , we extract features from layers `conv_3_3`, `conv_4_1`, `conv_4_3`, `head_1` and `head_3`, in the same setting as S2DHM, but using our trained localization head instead of the retrieval one. These features are upsampled to match with the resolution of the earliest layer (`conv_3_3` in this case, resolution is 1/4 of the input image) and concatenated. The result is the so called *hypercolumns* H_q and H_k , a dense descriptor that encodes information from different levels of the network.

As we have an available map, we will only try to match the 3D points P_k that were already detected in 2D locations $\{m_j^k\}_{j=1\dots P_k}$ in the keyframe. We interpolate the hypercolumn H_k at each location $\{m_j^k\}$, obtaining a sparse set of descriptors $\{d_j^k\}_{j=1\dots P_k}$. To find the matches between the dense query hypercolumn and the sparse keyframe descriptors, a dot product is computed between every sparse descriptor d_j^k and the dense hypercolumn, obtaining a cross-correlation map $C_{q,j}^k = H_q * d_j^k$. The tentative matches corresponds to the global maximum of the cross-correlation map for each of the points p_k considered. To avoid outliers due to repetitive patterns or occlusions, a ratio test is conducted.

The resulting P_k 2D-3D matches are fed into a PnP+RANSAC scheme, which outputs the final inliers and the initial pose estimation. The keyframe with the most inliers is the one selected, as well as the PnP pose estimated for the query. This estimation is the seed given to the final optimization.

D. Deep direct feature-metric image alignment

We employ the method proposed in [3] to align our hierarchy of deep features. As other recent works [4–6, 29], they treat deep image alignment as a direct feature-metric optimization problem, in a similar way as DSO [11]

minimizes the photometric error. We describe it briefly, for further details please refer to [3].

As PixLoc proposes, we extract $L=3$ feature maps from the UNet decoder, with strides 1, 4 and 16. The shallow levels encode low texture cues while deeper levels capture high level features and semantic content. This pyramidal representation is similar as what traditional photometric alignment uses. Learning this representation instead of relying on the raw photometric values allows to overcome with the known limitations of direct image alignment: illumination changes and small convergence basin.

For a feature level l , the feature-metric residual is defined as weighted addition of the feature-metric error between the query and the retrieved images for all the 3D map points, detected in the query image:

$$E_l(\mathbf{R}_q, \mathbf{t}_q) = \sum_{i,k} w_k^i \rho(\|\mathbf{r}_k^i\|_2^2) \quad (2)$$

$$\mathbf{r}_k^i = \mathbf{F}_q^l[\mathbf{p}_q^i] - \mathbf{F}_k^l[\mathbf{p}_k^i] \in \mathbb{R}^D \quad (3)$$

$$w_k^i = \frac{1}{1 + \mathbf{U}_q^l[\mathbf{p}_q^i]} \frac{1}{1 + \mathbf{U}_k^l[\mathbf{p}_k^i]} \in [0, 1]. \quad (4)$$

Where \mathbf{F}_q^l and \mathbf{F}_k^l are the feature maps for the query and the keyframe at a certain level l , $[\mathbf{p}_q^i]$ and $[\mathbf{p}_k^i]$ are the projections of the point \mathbf{P}_i with subpixel accuracy, and \mathbf{U}_q^l and \mathbf{U}_k^l are the predicted uncertainty maps. w_k^i learns to determine if the location of a 3D point is good for localization or not. If the point projection has low uncertainty in both the query and the reference image, w_k^i will tend to 1. Otherwise, w_k^i will tend to 0, weighting down the residual in the optimization. For N points, (2) defines the goal function to be minimized with the Levenberg-Marquadt (LM) algorithm. The network learns to find good features to localize and whether a point is reliable or not.

The initial guess for the iterative optimization is the one with the most inliers found by the Sparse-to-Dense matching. The algorithm starts optimizing the coarsest level (i.e. stride 16), the feature maps with lower resolution but higher depth, and successively optimizes the finer levels, going from an initial coarse estimation to a finer one. As the finer layer has the same resolution as the input image, feature-metric optimization can achieve subpixel accuracy, just like classic photometric alignment. The LM optimization for the camera pose comes down to solve the linear system:

$$(\mathbf{H} + \lambda \text{diag}(\mathbf{H})) \delta = \mathbf{J}^\top \mathbf{W} \mathbf{r} \quad (5)$$

$$\mathbf{H} = \mathbf{J}^\top \mathbf{W} \mathbf{J}, \quad (6)$$

where \mathbf{J} is the Jacobian, \mathbf{W} is weighting matrix depending on (4) and $\delta \in \mathbf{SE}(3)$ is the pose update of parameterized by its Lie algebra.

The damping parameter λ is formulated as a fixed 6×6 diagonal matrix coding the damping independently in each of the 6 DoF of the camera pose, these diagonal values are also learnt.

Loss function The only supervision for learning is the ground truth pose for the query images, $\{\bar{\mathbf{R}}_q, \bar{\mathbf{t}}_q\}$. The loss function penalizes the Huber cost of distance in pixels

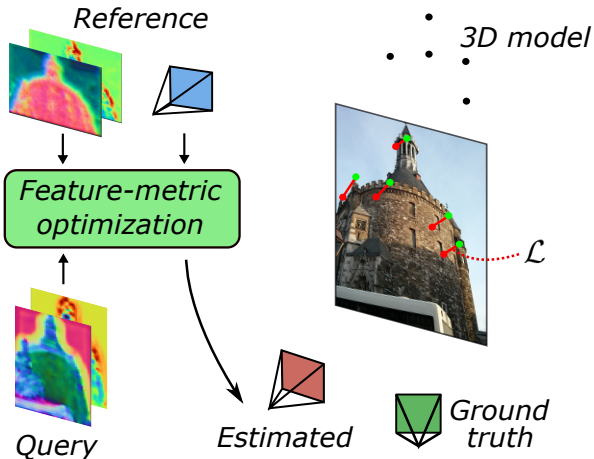


Fig. 4: Reprojection error loss. The training loss is computed by the reprojection loss between the projected 3D points with the ground truth pose (green dots) and the projection of the same points with the estimated pose after the optimization (red dots).

the between the reprojection of the map points in the ground camera pose (Figure 4), and the reprojections of the same points in the feature-metric optimized camera pose, $\{\mathbf{R}_{l,q}, \mathbf{t}_{l,q}\}$, averaging among the different scales.

$$\mathcal{L} = \frac{1}{L} \sum_l \sum_i \|\Pi(\mathbf{R}_{l,q} \mathbf{P}_i + \mathbf{t}_{l,q}) - \Pi(\bar{\mathbf{R}}_q \mathbf{P}_i + \bar{\mathbf{t}}_q)\|_\gamma, \quad (7)$$

This formulation is not affected by the geometric scale of the scene, as it only works with the reprojection of the points and not directly with camera poses.

IV. EXPERIMENTS

In this section we evaluate the advantages of our *retrieval deep alignment*, comparing it against other learned approaches. In section IV-A, we explain the datasets used for training and evaluation, and the baselines used to compare. We show the accuracy of the camera pose estimated by our system in large-scale visual localization in section IV-B, performing better than the other unified approaches and competitively against feature matching approaches. Finally, in section IV-C, we perform an ablation study, showing the benefits of each one of the elements of the pipeline.

A. Datasets and baselines

Training Our retrieval encoder is pretrained on SfM120k [1], which depicts common landmarks around the world, downloaded from Flickr and clustered with Structure-from-motion, using the contrastive loss and hard-negative mining for retrieval. We experimented with the original version given by the authors, which initializes their training with weights from custom ImageNet pretraining on Caffe [35], but we found better convergence and performance when initializing with PyTorch ImageNet pretraining. We use MegaDepth [36] dataset for training the feature-metric alignment procedure. It contains about 1M of images depicting popular landmarks,

Method	Aachen Day-Night		
	Day		Night
Pixloc	64.3 / 69.3 / 77.4	51.0 / 55.1 / 67.3	
S2DNet	84.3 / 90.9 / 95.9	46.9 / 69.4 / 86.7	
D2-Net	84.3 / 91.9 / 96.2	75.5 / 87.8 / 95.9	
hloc	89.6 / 95.4 / 98.8	86.7 / 93.9 / 100	
S2DHM	56.3 / 72.9 / 90.9	30.6 / 56.1 / 78.6	
HF-Net	79.9 / 88.0 / 93.4	40.8 / 56.1 / 74.5	
UR2KiD	79.9 / 88.6 / 93.6	45.9 / 64.3 / 83.7	
DRAN (ours)	77.9 / 87.0 / 90.9	67.3 / 75.5 / 85.7	

TABLE I: Results for Aachen Day-Night.

grouped into 196 scenes and reconstructed by COLMAP [37]. MegaDepth provides depth maps and pose information for every camera. We use the same split as D2-Net [24] for training and validation. The training is performed for 20k iterations with the Adam optimizer, using a constant learning rate of 5×10^{-6} and a batch size of 6.

Evaluation We selected Aachen Day-Night for evaluation, as it depicts the old inner city of Aachen, testing visual localization under day-night condition. Aachen Day-Night include SfM reconstructions: 3D point clouds/dense maps and camera poses. As proposed by [1], we use multiscale and learned whitening to obtain the retrieval candidates, for scales 1, $\frac{1}{\sqrt{2}}$ and $\frac{1}{2}$.

Baselines We compare against two groups of methods: Feature Matching (FM) and Unified methods.

For Feature Matching, we consider methods for matching between two images, where the image retrieval is given as external prior. In this group we found the state-of-the-art methods for local matching as D2-Net [24] or the toolbox hloc [25, 26], which uses SuperPoint [23] and SuperGlue [26]. We also compare against PixLoc [3], which performs feature-metric optimization, and S2DNet [30], a matching system for sparse-to-dense matching.

In the Unified methods, we consider methods able to perform retrieval and recover a 6DoF pose with a single network. Here we found S2DHM [34], which performs sparse-to-dense matching with an encoder trained for retrieval in a subset of RobotCar Seasons and HF-Net [25], a pipeline that distilled knowledge from NetVLAD [2] and SuperPoint [23] in a compact network. UR2KiD[33] is also considered, as it is able to perform retrieval and local matching while only being trained with image to image matches but not in image to map matches.

B. Large-scale localization

Aachen Day-Night objective is to evaluate visual localization under challenging conditions. It is composed of 4,328 references images depicting the city of Aachen, taken during daytime with hand-held devices. A 3D model is reconstructed with these images, and 922 queries (824 daytime, 98 nighttime) along with its 6DoF are provided. The benchmark protocol from [38] report the percentage

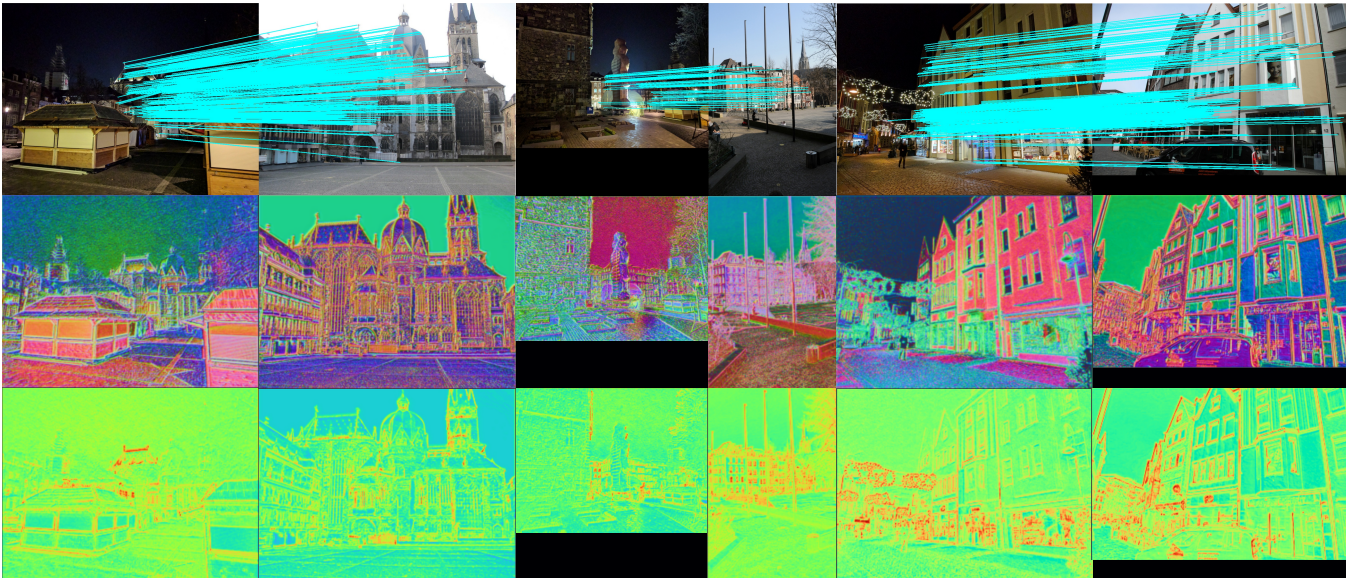


Fig. 5: Examples from Aachen Day-Night. Each two columns depicts a query-reference pair. The first row shows the Sparse-to-Dense matching of our approach, showing impressive results in night conditions under severe viewpoint change or occlusions. The second row shows the features \mathbf{F} from the finest resolution learned in the decoder. The last row shows the also learned uncertainty maps \mathbf{U} , where red means that points are more reliable, and blue that points are ignored.

of queries localized for different thresholds for the camera position and orientation error. Localization recall is provided for three threshold levels: (25cm, 2°), (50cm, 5°) and (5m, 10°), which can be seen in Table I.

Among the unified approaches, DRAN performs the best by a great margin in the night-queries, while performing comparably as UR2KiD in the day ones. Feature matching pipelines as hloc, that uses NetVLAD, SuperPoint and SuperGlue, are more robust and precise than ours, with the drawback that they use several networks to perform localization, while we only need one. DRAN obtains the camera pose estimation using the top-3 candidates in the initial retrieval list.

Aachen Day-Night reference poses are really sparse, providing an extremely coarse initialization that makes difficult to pure feature-metric methods to converge. Here is where the sparse-to-dense method shines, finding matches in difficult situations (Figure 5) and providing an initial pose much more precise to the feature-metric optimization. In contrast to PixLoc, which only performs the optimization with a given retrieval, we are able to perform our own retrieval and estimate more accurate and robust camera poses.

C. Ablation study

We perform an ablation study of the different modules of our algorithm (Table II.) Using our top scored keyframe of our retrieval network (R) as the initial guess for deep image alignment (A), gives similar results on the day to Pixloc, the most comparable method, but improves by an average of 10% in the night queries.

Performing retrieval and only PnP with hypercolumns (R+P) allows to produce an accurate pose by itself giving a huge boost to the performance. Having an encoder trained

Method	Aachen Day-Night	
	Day	Night
DRAN (R+A)	62.5 / 69.2 / 76.9	58.2 / 62.2 / 70.4
DRAN (R+P)	73.4 / 83.3 / 90.8	63.3 / 74.5 / 85.7
DRAN (R+P+A)	77.9 / 87.0 / 90.9	67.3 / 75.5 / 85.7

TABLE II: Ablation study in Aachen Day-Night.

in a generic retrieval dataset is beneficial for generalization, specially in the night case, where DRAN doubles the recall of S2DHM, which was trained on RobotCar Seasons.

Finally, using all the above modules (R+P+A), where the feature-metric optimization uses R+P as initial guess conforms a unified pipeline that beats the state-of-the-art of multitasks methods in Aachen night queries, while being competitive on the day condition. In Figure 6, we show an example where DRAN can not converge using (R+A), but successfully localizes with the full method (R+P+A), showing the increase in robustness.

D. Implementation

For the feature-metric optimization and training, we built DRAN upon the original implementation of PixLoc, bringing there the retrieval and sparse-to-dense ideas.

Running on a PC with a Intel® Core™ i7-10700K (3.80GHz) CPU and an Nvidia GeForce RTX 2080 Ti, the typical times for one image with 2000 points are 300ms for the extraction, 700ms for the sparse-to-dense matching and between 200 to 400ms for the feature-metric optimization. The ratio test method is the current bottleneck, averaging 0.36ms per point. This is not optimized and could be substituted by a non-maxima suppression method on GPU.

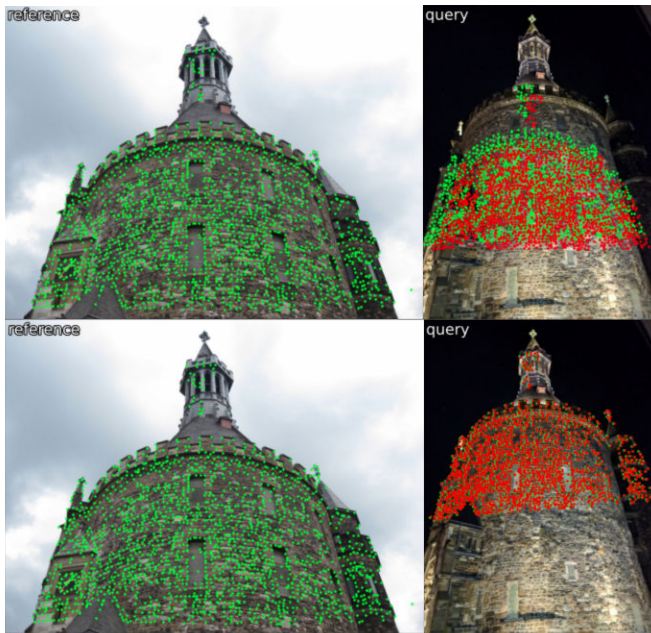


Fig. 6: The Sparse-to-Dense module allows convergence when reference poses are sparse. Left column: reference image along with the 3D points that it observes (shown in green). Right column: query image with points reprojected using the initial pose (red points) and the optimized (green). With retrieval initialization (top row) the optimization does not converge, while with PnP pose (bottom row) it does.

V. CONCLUSIONS

We have presented a unified pipeline that performs all the tasks concerning Visual Localization under challenging conditions. Compared with other approaches in Aachen, DRAN, not only is competitive in day conditions to feature matching pipelines that are not able to perform retrieval by themselves, but also improves state-of-the-art in night queries among the other unified approaches. In our opinion, SLAM pipelines should have a unique feature extractor, able to provide good features for tracking and relocalization. We see DRAN as a first step towards that paradigm. As a future work, we would consider extending DRAN to other datasets and to train jointly the tasks of retrieval and camera pose estimation.

REFERENCES

- [1] F. Radenović, G. Tolias, and O. Chum, “Fine-tuning cnn image retrieval with no human annotation,” *IEEE transactions on pattern analysis and machine intelligence*, vol. 41, no. 7, pp. 1655–1668, 2018.
- [2] R. Arandjelovic, P. Gronat, A. Torii, T. Pajdla, and J. Sivic, “Netvlad: Cnn architecture for weakly supervised place recognition,” in *Proceedings of the IEEE conference on computer vision and pattern recognition*, 2016, pp. 5297–5307.
- [3] P.-E. Sarlin, A. Unagar, M. Larsson, H. Germain, C. Toft, V. Larsson, M. Pollefeys, V. Lepetit, L. Hammarstrand, F. Kahl, *et al.*, “Back to the future: Learning robust camera localization from pixels to pose,” in *Proceedings of the IEEE/CVF Conference on Computer Vision and Pattern Recognition*, 2021, pp. 3247–3257.
- [4] L. Von Stumberg, P. Wenzel, Q. Khan, and D. Cremers, “Gn-net: The gauss-newton loss for multi-weather relocalization,” *IEEE Robotics and Automation Letters*, vol. 5, no. 2, pp. 890–897, 2020.
- [5] L. Von Stumberg, P. Wenzel, N. Yang, and D. Cremers, “Lm-reloc: Levenberg-marquardt based direct visual relocalization,” in *2020 International Conference on 3D Vision (3DV)*, IEEE, 2020, pp. 968–977.
- [6] Z. Lv, F. Dellaert, J. M. Rehg, and A. Geiger, “Taking a deeper look at the inverse compositional algorithm,” in *Proceedings of the IEEE/CVF Conference on Computer Vision and Pattern Recognition*, 2019, pp. 4581–4590.
- [7] R. Mur-Artal, J. M. M. Montiel, and J. D. Tardos, “Orb-slam: A versatile and accurate monocular slam system,” *IEEE transactions on robotics*, vol. 31, no. 5, pp. 1147–1163, 2015.
- [8] C. Campos, R. Elvira, J. J. G. Rodríguez, J. M. Montiel, and J. D. Tardós, “ORB-SLAM3: An accurate open-source library for visual, visual-inertial, and multimap slam,” *IEEE Transactions on Robotics*, 2021.
- [9] A. J. Davison, I. D. Reid, N. D. Molton, and O. Stasse, “Monoslam: Real-time single camera slam,” *IEEE transactions on pattern analysis and machine intelligence*, vol. 29, no. 6, pp. 1052–1067, 2007.
- [10] G. Klein and D. Murray, “Parallel tracking and mapping for small ar workspaces,” in *2007 6th IEEE and ACM international symposium on mixed and augmented reality*, IEEE, 2007, pp. 225–234.
- [11] J. Engel, V. Koltun, and D. Cremers, “Direct sparse odometry,” *IEEE transactions on pattern analysis and machine intelligence*, vol. 40, no. 3, pp. 611–625, 2017.
- [12] J. Engel, T. Schöps, and D. Cremers, “Lsd-slam: Large-scale direct monocular slam,” in *European conference on computer vision*, Springer, 2014, pp. 834–849.
- [13] R. A. Newcombe, S. J. Lovegrove, and A. J. Davison, “Dtam: Dense tracking and mapping in real-time,” in *2011 international conference on computer vision*, IEEE, 2011, pp. 2320–2327.
- [14] D. G. Lowe, “Distinctive image features from scale-invariant keypoints,” *International journal of computer vision*, vol. 60, no. 2, pp. 91–110, 2004.
- [15] E. Rublee, V. Rabaud, K. Konolige, and G. Bradski, “Orb: An efficient alternative to sift or surf,” in *2011 International conference on computer vision*, Ieee, 2011, pp. 2564–2571.

- [16] D. Nister and H. Stewenius, "Scalable recognition with a vocabulary tree," in *2006 IEEE Computer Society Conference on Computer Vision and Pattern Recognition (CVPR'06)*, vol. 2, 2006, pp. 2161–2168. DOI: 10.1109/CVPR.2006.264.
- [17] D. Gálvez-López and J. D. Tardós, "Bags of binary words for fast place recognition in image sequences," *IEEE Transactions on Robotics*, vol. 28, no. 5, pp. 1188–1197, Oct. 2012, ISSN: 1552-3098. DOI: 10.1109/TRO.2012.2197158.
- [18] J. Revaud, J. Almazán, R. S. Rezende, and C. R. d. Souza, "Learning with average precision: Training image retrieval with a listwise loss," in *Proceedings of the IEEE/CVF International Conference on Computer Vision*, 2019, pp. 5107–5116.
- [19] F. Radenović, G. Toliás, and O. Chum, "Cnn image retrieval learns from bow: Unsupervised fine-tuning with hard examples," in *European conference on computer vision*, Springer, 2016, pp. 3–20.
- [20] M. Teichmann, A. Araujo, M. Zhu, and J. Sim, "Detect-to-retrieve: Efficient regional aggregation for image search," in *Proceedings of the IEEE/CVF Conference on Computer Vision and Pattern Recognition*, 2019, pp. 5109–5118.
- [21] A. Kendall and R. Cipolla, "Geometric loss functions for camera pose regression with deep learning," in *Proceedings of the IEEE conference on computer vision and pattern recognition*, 2017, pp. 5974–5983.
- [22] T. Naseer and W. Burgard, "Deep regression for monocular camera-based 6-dof global localization in outdoor environments," in *2017 IEEE/RSJ International Conference on Intelligent Robots and Systems (IROS)*, IEEE, 2017, pp. 1525–1530.
- [23] D. DeTone, T. Malisiewicz, and A. Rabinovich, "Superpoint: Self-supervised interest point detection and description," in *Proceedings of the IEEE conference on computer vision and pattern recognition workshops*, 2018, pp. 224–236.
- [24] M. Dusmanu, I. Rocco, T. Pajdla, M. Pollefeys, J. Sivic, A. Torii, and T. Sattler, "D2-net: A trainable cnn for joint description and detection of local features," in *Proceedings of the IEEE/CVF conference on computer vision and pattern recognition*, 2019, pp. 8092–8101.
- [25] P.-E. Sarlin, C. Cadena, R. Siegwart, and M. Dymczyk, "From coarse to fine: Robust hierarchical localization at large scale," in *Proceedings of the IEEE/CVF Conference on Computer Vision and Pattern Recognition*, 2019, pp. 12 716–12 725.
- [26] P.-E. Sarlin, D. DeTone, T. Malisiewicz, and A. Rabinovich, "Superglue: Learning feature matching with graph neural networks," in *Proceedings of the IEEE/CVF conference on computer vision and pattern recognition*, 2020, pp. 4938–4947.
- [27] J. Sun, Z. Shen, Y. Wang, H. Bao, and X. Zhou, "Loftr: Detector-free local feature matching with transformers," in *Proceedings of the IEEE/CVF Conference on Computer Vision and Pattern Recognition*, 2021, pp. 8922–8931.
- [28] V. Lepetit, F. Moreno-Noguer, and P. Fua, "EPnP: An accurate o (n) solution to the PnP problem," *International journal of computer vision*, vol. 81, no. 2, p. 155, 2009.
- [29] B. Xu, A. J. Davison, and S. Leutenegger, "Deep probabilistic feature-metric tracking," *IEEE Robotics and Automation Letters*, vol. 6, no. 1, pp. 223–230, 2020.
- [30] H. Germain, G. Bourmaud, and V. Lepetit, "S2dnet: Learning image features for accurate sparse-to-dense matching," in *European Conference on Computer Vision*, Springer, 2020, pp. 626–643.
- [31] B. Cao, A. Araujo, and J. Sim, "Unifying deep local and global features for image search," in *European Conference on Computer Vision*, Springer, 2020, pp. 726–743.
- [32] H. Noh, A. Araujo, J. Sim, T. Weyand, and B. Han, "Large-scale image retrieval with attentive deep local features," in *Proceedings of the IEEE international conference on computer vision*, 2017, pp. 3456–3465.
- [33] T.-Y. Yang, D.-K. Nguyen, H. Heijnen, and V. Balntas, "Ur2kid: Unifying retrieval, keypoint detection, and keypoint description without local correspondence supervision," *arXiv preprint arXiv:2001.07252*, 2020.
- [34] H. Germain, G. Bourmaud, and V. Lepetit, "Sparse-to-dense hypercolumn matching for long-term visual localization," in *2019 International Conference on 3D Vision (3DV)*, IEEE, 2019, pp. 513–523.
- [35] Y. Jia, E. Shelhamer, J. Donahue, S. Karayev, J. Long, R. Girshick, S. Guadarrama, and T. Darrell, "Caffe: Convolutional architecture for fast feature embedding," *arXiv preprint arXiv:1408.5093*, 2014.
- [36] Z. Li and N. Snavely, "Megadepth: Learning single-view depth prediction from internet photos," in *Proceedings of the IEEE Conference on Computer Vision and Pattern Recognition*, 2018, pp. 2041–2050.
- [37] J. L. Schonberger and J.-M. Frahm, "Structure-from-motion revisited," in *Proceedings of the IEEE conference on computer vision and pattern recognition*, 2016, pp. 4104–4113.
- [38] T. Sattler, W. Maddern, C. Toft, A. Torii, L. Hammarstrand, E. Stenborg, D. Safari, M. Okutomi, M. Pollefeys, J. Sivic, *et al.*, "Benchmarking 6dof outdoor visual localization in changing conditions," in *Proceedings of the IEEE conference on computer vision and pattern recognition*, 2018, pp. 8601–8610.